TÜBİTAK

Turkish Journal of Chemistry

http://journals.tubitak.gov.tr/chem/

Research Article

Turk J Chem
(2015) 39: 734 – 749

doi:10.3906/kim-1412-64

Optimization of the adsorption of a textile dye onto nanoclay using a central composite design

Aydin HASSANI[1,*], Murat KIRANŞAN[1], Reza DARVISHI CHESHMEH SOLTANI[2], Alireza KHATAEE[3], Semra KARACA[1,*]

[1]Department of Chemistry, Faculty of Science, Atatürk University, Erzurum, Turkey

[2]Department of Environmental Health Engineering, School of Health, Arak University of Medical Sciences, Arak, Iran

[3]Research Laboratory of Advanced Water and Wastewater Treatment Processes, Department of Applied Chemistry, Faculty of Chemistry, University of Tabriz, Tabriz, Iran

Received: 25.12.2014 • **Accepted/Published Online:** 16.04.2015 • **Printed:** 28.08.2015

Abstract: The main aim of this study was to evaluate the efficacy of montmorillonite clay for the adsorption of C.I. Basic Yellow 2 (BY2) dye from aqueous media. The experimental results were processed by response surface methodology based on a central composite design (CCD). The effect of four main variables, including initial BY2 concentration, adsorbent dosage, reaction time, and temperature on the removal of BY2 was evaluated by the model. The accuracy of the model and regression coefficients was appraised by employing analysis of variance. The results demonstrated a good agreement between the predicted values obtained by the model and the experimental values ($R^2 = 0.972$). Accordingly, the maximum BY2 removal of 97.32% was achieved with an initial BY2 concentration of 60 mg/L, adsorbent dosage of 0.6 g/L, reaction time of 10 min, and initial temperature of 25 °C. The results demonstrated the high efficiency of montmorillonite clay for the adsorption of BY2 dye from aqueous solution based on the data processed by CCD approach. The adsorbent dosage was found to be the key factor that controlled dye adsorption. The adsorption kinetic and isotherm were also investigated. The rate of adsorption showed the best fit with the pseudo-second order model ($R^2 = 1$). The results of the isotherm study fit the Freundlich model ($R^2 > 0.9$). The physicochemical properties of the sample were determined by XRF, XRD, FT-IR, and N_2 adsorption–desorption.

Key words: Adsorption, central composite design, experimental design, montmorillonite K10, nanoclay

1. Introduction

The presence of organic dyes in aqueous environments such as rivers and lakes can cause detrimental effects on such environments due to the reduction in light penetration and photosynthesis. Moreover, the presence of dyes in aqueous environments adversely affects their aesthetic nature.[1] There are many technologies to remove organic dyes from industrial effluents including biological, adsorption, membrane, coagulation–flocculation, ozonation, and advanced oxidation processes.[2,3] Because of the low biodegradability of organic dyes, conventional biological treatments are not efficient enough to degrade organic dyes and treat colored wastewaters; thus, organic dyes in aqueous solutions are degraded or removed through physicochemical processes.[3,4] Among the physicochemical treatment methods, adsorption using solid adsorbent has been found to be efficient and economical.[5–7] However, using activated carbon, the most widely used adsorbent, has become limited because

*Correspondence: aydin_hassani@yahoo.com, semra_karaca@yahoo.com

of its high capital and operational costs.[8,9] Therefore, there is a growing demand to develop new materials for sequestering organic dyes from aqueous media. In recent decades, natural clay materials have been widely used for removing organic compounds such as organic dyes from aqueous solutions because of their availability, nontoxicity, mechanical and chemical stabilities, high surface area, and low price compared to the conventional activated carbon.[10,11] Montmorillonite is one type of clay material, existing in most soils abundantly. This type of clay is employed as a low-cost alternative to activated carbon.[12] Thus, in recent years, the application of montmorillonite for treating polluted aqueous environments has been widely investigated by many researchers.[13–16] Based on the above-mentioned statements, in the present study, montmorillonite of nanosize named nanoclay was considered for the adsorption of Basic Yellow 2 (BY2) dye from aqueous solutions. The characteristics of nanoclay were firstly assessed by X-ray diffraction (XRD), Fourier transform infrared spectra (FT-IR), X-ray fluorescence (XRF), and Brunauer–Emmett–Teller (BET) analysis and then used for the adsorption of C.I. BY2 as an azo dye from aqueous solutions. To vigorously evaluate the potential of montmorillonite for the adsorption of BY2, response surface methodology (RSM) based on a central composite design (CCD) was employed to investigate the effect of four main operational parameters influencing the decolorization of BY2: initial dye concentration, adsorbent dosage, temperature, and reaction time. Nowadays, process optimization is proposed as a beneficial tool for discovering conditions in which the best possible response can be obtained. RSM is an empirical designing, modeling, and optimizing technique for evaluating the influence of independent parameters and their interactive effects on responses with a reduced number of experiments. Already, the RSM approach has been successfully used to optimize response efficiency and evaluate simple and combined effects of different operational parameters on the removal of dye via different treatment processes.[10,17–19] RSM is an effective experimental design approach to predict the efficiency of an experimental system. Using RSM, various parameters are simultaneously examined with a minimum number of experiments, demonstrating that the study processed by RSM is less expensive and time consuming than the conventional one-factor-at-a-time statistical strategy.

2. Results and discussion

2.1. Structural characteristics

2.1.1. XRD analysis

XRD analysis was performed to study the structural characteristics of the nanoclay. As illustrated in Figure 1, five narrow peaks of the studied montmorillonite are located at 19.84, 26.65, 34.93, 61.66, and 73.05°, indicating the montmorillonite clay is crystalline in nature. MMT in a 2:1 layer structure has ability to swell. The basal spacing of this phase was significantly enlarged by pretreatment as a result of this swelling feature.[17,20] Interlayer spacing of MMT was quantitatively assessment using the Debye–Scherrer equation $d = (k\lambda/\beta\cos\theta)$. In this equation d is the thickness of the crystal, k is the Debye–Scherrer constant (0.89), k is the X-ray wavelength (0.15406 nm), b is width of the peak with the maximum intensity in half height, and h is the diffraction angle.[21] The result obtained from analyses of the XRD pattern by using the Debye–Scherrer equation indicated that the interlayer spacing of MMT ($2\theta = 26.65°$) was about 29 nm.

2.1.2. BET analysis

In order to obtain the surface area of the nanoclay, N_2 adsorption and desorption were carried out at 77 K and plotted as adsorbed volume versus relative pressure (Figure 2). The surface areas and pore size distributions were calculated using BET and Barrett–Joyner–Halenda (BJH) desorption in the range of 1.5–100 nm. The results are given in Table 1. The obtained adsorption isotherm matches well the Type II isotherm as

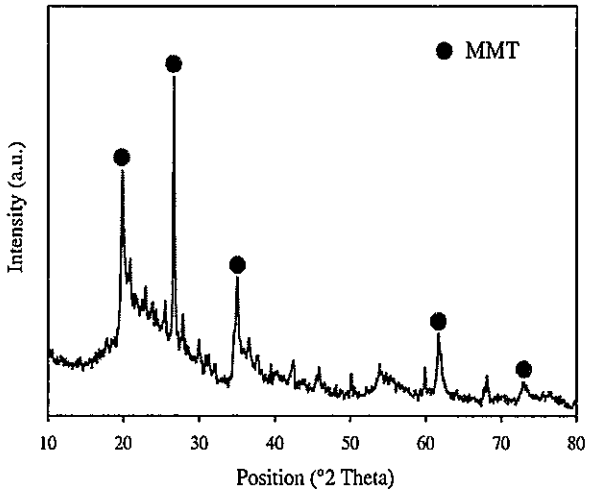

Figure 1. XRD pattern of the montmorillonite nanoclay.

classified by the IUPAC.[22] This type of isotherm relates to multilayer physical adsorption and describes strong interactions between adsorbate and adsorbent. The isotherm of clay (Figure 2) shows a type-H4 hysteresis loop, revealing that the sample has a mesoporous texture containing open slit-shaped capillaries.[23] The adsorption–desorption hysteresis on the clay sample isotherm showed clearly that liquid nitrogen was condensed in slit-shaped mesopores.[24] The inset of Figure 2 is the pore size distributions of the clay sample used in this study, in which different volume is plotted against pore size for the desorption branches of the N_2 adsorption–desorption isotherms according to the BJH model.[25] The total pore volume and average pore radius were 0.416 cm^3/g and 3.17 nm, respectively. The BJH adsorption cumulative surface area of pores was 287.7 m^2/g and BJH cumulative pore volume was 0.456 cm^3/g. The calculated monolayer adsorption capacity of clay using the BET and Langmuir equation were 64.1548 cm^3/g, STP and 88.6608 cm^3/g, STP, respectively.[26] The obtained q_m values for the Langmuir isotherm are higher than those of the BET isotherm, implying that the clay sample is a heteroporous material exhibiting microporous properties.

Table 1. Summary of physicochemical characterization of montmorillonite K10.

Parameter	Value
BET surface area (m^2/g)	279.27
BJH pore volume (cm^3/g)	0.456
BJH pore radius (nm)	3.17
Total pore volume (cm^3/g)	0.416
Average pore width (nm)	5.97
Internal surface area (m^2/g)	6.67
External surface area (m^2/g)	272.60

2.1.3. FT-IR analysis

FT-IR analysis was conducted to evaluate the involvement of surficial functional groups in the adsorption of BY2 onto nanoclay. The FT-IR spectra of pure clay and the dye adsorbed nanoclay sample are shown in Figure 3. The FT-IR spectra of MMT (Figure 3) showed a broad band centered near 3395 cm^{-1} due to a

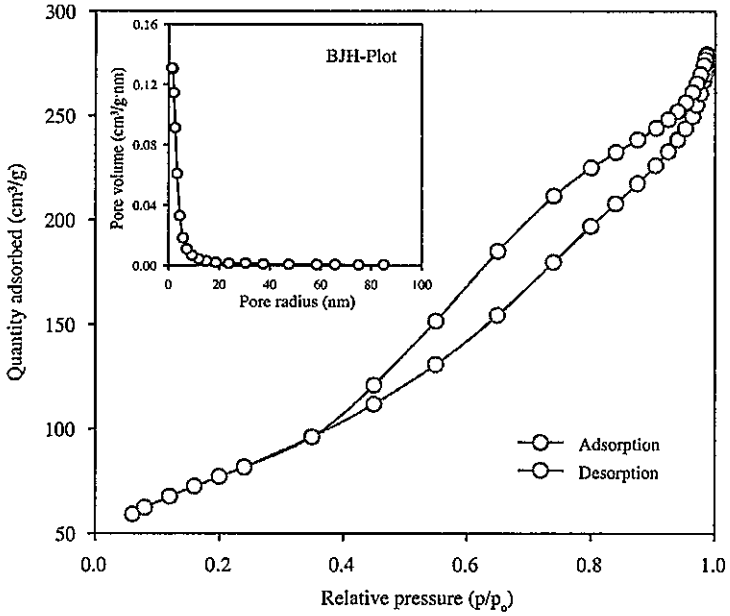

Figure 2. N_2 adsorption–desorption isotherms and pore size distribution of the montmorillonite K10.

–OH stretching band for interlayer water. The bands at 3600 and 3649 cm^{-1} are due to OH stretching of structural hydroxyl groups.[6,27,28] The shoulders and broadness of the structural –OH band are mainly due to contributions of several structural –OH groups occurring in the clay mineral. The absorption band in the region of 1670 cm^{-1} is attributed to the –OH bending mode of adsorbed water. The characteristic peak at 1110 cm^{-1} is the Si–O stretching (out-of-plane) band. A strong peak appearing at 1030 cm^{-1} is indicative of the presence of Si–O–Si stretching (in-plane) vibration for layered silicates.[29,30] The bands at 937, 702, 537, and 477 cm^{-1} are attributed to Al–Al–OH, Mg–OH, Si–O–Al, and Si–O–Mg bending vibrations, respectively.[31] The presence of various binding groups on the surface of adsorbent, especially ionizable –OH groups, would be beneficial for the adsorption of cationic species such as BY2.[28] It can be observed that the intensity of the peak associated with the –OH group diminished after the adsorption of BY2, which confirmed the significant role of this peak in the adsorption process. Compared to MMT, the spectra of dye-loaded clay showed two additional peaks at 1418 and 1514 cm^{-1}, which were attributed to the CH bending of alkene (in plane) and N–H bending vibrations, respectively. This indicated the incorporation of dye in the structure of nanoclay after the adsorption process. The shift of bands belonging to Si–O and all of –OH vibrations and/or change in their intensities imply the presence of strong electrostatic interactions and also hydrogen bonds between dye molecules and these functional groups.[32] The –OH plays a significant role for the adsorption of adsorbate molecules via hydrogen bonding.[33] Conclusively, the results of FT-IR analysis suggested that BY2 is held onto nanoclay by chemical activation, indicating dye/nanoclay complexation.[14] Similar results were reported by Malkoç et al.[34]

2.2. Model results for the removal of BY2 by montmorillonite

An empirical mutual relationship between the response (CR (%)) and independent studied variables was obtained using Design-Expert software and is shown through Eq. (1):

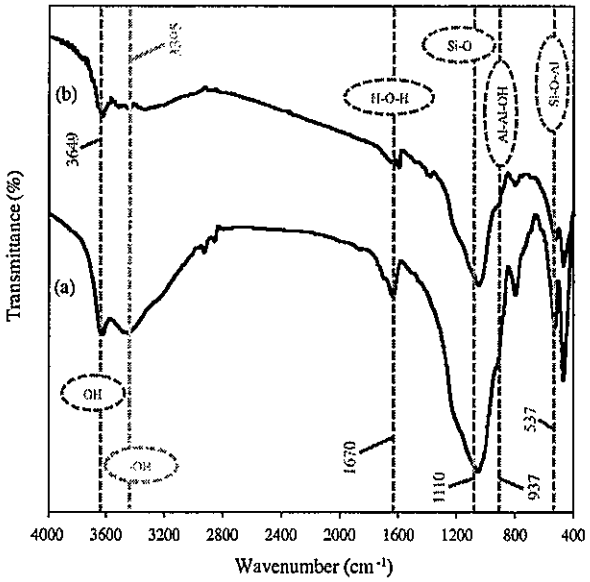

Figure 3. FT-IR spectra of the nanoclay before (a) and after (b) adsorption of dye.

$$\begin{aligned} Y(CR(\%)) &= 98.78 - 0.82x_1 + 1.68x_2 - 0.063x_3 + 0.047x_4 + 1.13x_1x_2 + 0.023x_1x_3 - 0.015x_1x_4 \\ &\quad -0.18x_2x_3 - 0.085x_2x_4 + 0.026x_3x_4 - 0.44x_{12} - 0.91x_{22} + 0.022x_{32} - 0.043x_{42} \end{aligned} \quad (1)$$

Accordingly, the experimental and predicted CR values (%) are shown in Table 2. One of the most important approaches to test the adequacy and reliability of the statistical model is performing analysis of variance (ANOVA);[18,35] thus, ANOVA was performed for the adsorption of BY2 onto nanoclay and the results are provided in Table 3. In this manner, the significance and suitability of the model were determined by the obtained correlation coefficient (R^2) and adjusted R^2 between the experimental and predicted values of the CR (%). The closer the correlation coefficient value is to 1, the better it predicts the determined response. The correlation coefficient (R^2) and corresponding adjusted R^2 were calculated via Eqs. (2) and (3):[36]

$$R^2 = 1 - \frac{SS_{residual}}{SS_{model} - SS_{residual}} \quad (2)$$

$$R^2_{adj} = 1 - \frac{n-1}{(n-p)(1-R^2)}, \quad (3)$$

where SS, n, and p are the sum of the squares, the number of experiments, and the number of predictors in the model, respectively. Figure 4a shows good agreement between the predicted and experimental results (R^2 = 0.972), indicating the significance of the model applied for the adsorption of BY2 onto montmorillonite. An obtained correlation coefficient of 0.972 indicates that 97.2% of the variations for BY2 removal (%) are explained by the applied model and the model does not explain only 2.8% of the variations. Adjusted R^2 is also a good tool to check the adjustment of the experimental results to the predicted values. The adjusted R^2 corrects the value of R^2 for the sample size and the number of terms by way of the degrees of freedom on its computations. Having many terms in a model along with not very large sample size results in a smaller adjusted R^2 compared to the value of R^2.[37] According to Table 3, the value of adjusted R^2 was 0.949. Therefore, it seems that there

Table 2. Experimental and predicted results of the CCD model for the adsorption of BY2 by montmorillonite.

Run	Coded variable				Actual variable				Removal efficiency (%)	
order	X1	X2	X3	X4	X1	X2	X3	X4	Experimental	Predicted
1	1	1	−1	1	80	1.15	30	35	99.18	99.53
2	1	1	1	1	80	1.15	50	35	99.08	99.14
3	0	0	0	0	60	0.80	40	25	98.55	98.77
4	−1	1	−1	−1	40	1.15	30	15	99.38	99.09
5	0	0	0	0	60	0.80	40	25	98.79	98.77
6	1	1	−1	−1	80	1.15	30	15	99.10	99.68
7	0	0	0	2	60	0.80	40	45	98.61	98.69
8	2	0	0	0	100	0.80	40	25	96.39	95.35
9	1	1	1	−1	80	1.15	50	15	98.69	99.19
10	0	0	2	0	60	0.80	60	25	99.04	98.73
11	−1	−1	−1	−1	40	0.45	30	15	97.31	97.45
12	0	0	0	0	60	0.80	40	25	98.78	98.77
13	−1	1	1	1	40	1.15	50	35	98.38	98.51
14	0	0	0	−2	60	0.80	40	5	98.91	98.50
15	0	0	0	0	60	0.80	40	25	98.85	98.77
16	−1	−1	1	−1	40	0.45	50	15	97.83	97.58
17	−1	−1	−1	1	40	0.45	30	35	98.09	97.69
18	0	0	0	0	60	0.80	40	25	98.74	98.77
19	0	0	0	0	60	0.80	40	25	98.93	98.77
20	1	−1	−1	1	80	0.45	30	35	93.59	93.72
21	1	−1	1	−1	80	0.45	50	15	93.40	93.76
22	−1	1	−1	1	40	1.15	30	35	99.16	98.99
23	−1	1	1	−1	40	1.15	50	15	98.44	98.50
24	0	−2	0	0	60	0.10	40	25	91.62	91.78
25	−2	0	0	0	20	0.80	40	25	97.92	98.64
26	−1	−1	1	1	40	0.45	50	35	98.32	97.93
27	0	0	0	0	60	0.80	40	25	98.76	98.77
28	1	−1	1	1	80	0.45	50	35	93.66	94.05
29	0	0	−2	0	60	0.80	20	25	99.00	98.98
30	1	−1	−1	−1	80	0.45	30	15	93.57	93.54
31	0	2	0	0	60	1.50	40	25	98.98	98.50

is not a significant difference between R^2 and corresponding adjusted R^2. This indicates a good fit between the predicted results by the models and corresponding experimental results. As given in Table 3, "adequate precision" measures the difference between the signal and the noise (signal-to-noise ratio), and a ratio of greater than 4 is favorable.[10,18] Therefore, the obtained precision of 23.53 indicates an adequate signal. In addition, a very low value of the coefficient of variation (CV = 0.49%) demonstrates good reliability of the model for predicting the color removal (%) under different operational conditions.[18] Moreover, the adequacy of the model can be determined by the residuals calculated through determining the difference between the experimental and the predicted color removal.[38] Figure 4b depicts the normal probability (%) versus residuals for removing BY2 by montmorillonite. The normal probability plot determines normal distribution of the residuals. Figure 4b shows that the obtained data points appear on a straight trend line without considerable dispersal, indicating

the suitability of the model with low residual values. Moreover, the residuals were plotted versus the predicted CR (%) (Figure 4c) and the run number (Figure 4d) in which a random dispersal of the residuals was obtained for each plot. In addition, the significance and adequacy of the model can be checked by F-value and P-value. A larger F-value together with a smaller P-value indicates the suitability of the models.[19] An F-value of 40.73 and a P-value of <0.0001 demonstrated the adequacy of the model for predicting the BY2 removal (%) as response (Table 3). P-values less than 0.05 indicate that model terms are significant and values greater than 0.10 indicate an insignificant model. Moreover, the F- and P-values are good tools to check the importance of each variable or the interactions between the variables.[35] As listed in Table 4, among the studied variables, the adsorbent dosage (b_1) with an F-value greater than 290 and P-value smaller than 0.0001 produced the maximum effect on BY2 removal (%). In addition, the BY2 removal (%) is evidently influenced by the initial BY2 concentration (b_2), in the second place, with an F-value greater than 69 and a P-value smaller than 0.0001. However, the effects of the temperature (F-value = 0.40) and the reaction time (F-value = 0.23) are lower compared to those of the other two variables.

Table 3. Analysis of variance (ANOVA) for the adsorption of BY2 onto montmorillonite.

Source	Sum of squares	Degree of freedom	Mean square	F-value	P-value
Regression	133.08	14	9.51	40.73	< 0.0001
Residuals	3.73	16	0.23		
Pure error	0.081		0.013		
Total	136.81	30			

R^2 = 0.972, adjusted R^2 = 0.949, adequate precision = 23.53, coefficient of variation (CV) = 0.49 (%).

Table 4. Estimated regression coefficient and corresponding F and P values obtained by central composite design for the adsorption of BY2.

Coefficient	Coefficient estimate	Standard error	F-value	P-value
b_0	98.78	0.180	40.73	0.0001
b_1	–0.82	0.099	69.29	0.0001
b_2	1.680	0.099	290.82	0.0001
b_3	–0.063	0.099	0.40	0.5352
b_4	0.047	0.099	0.23	0.6366
b_{12}	1.130	0.120	86.96	0.0001
b_{13}	0.023	0.120	0.035	0.8546
b_{14}	–0.015	0.120	0.015	0.9027
b_{23}	–0.18	0.120	2.22	0.1556
b_{24}	–0.085	0.120	0.50	0.4917
b_{34}	0.026	0.120	0.047	0.8307
b_{11}	–0.44	0.090	24.23	0.0002
b_{22}	–0.91	0.090	101.12	0.0001
b_{33}	0.022	0.090	0.057	0.8145
b_{44}	–0.043	0.090	0.23	0.6370

2.3. Interactive effects of the studied variables

The response surface and contour plots can be used to assess CR (%) according to a polynomial function. In this approach, two variables were constant and the other two variables would be varied.[2,38,39] The three-dimensional

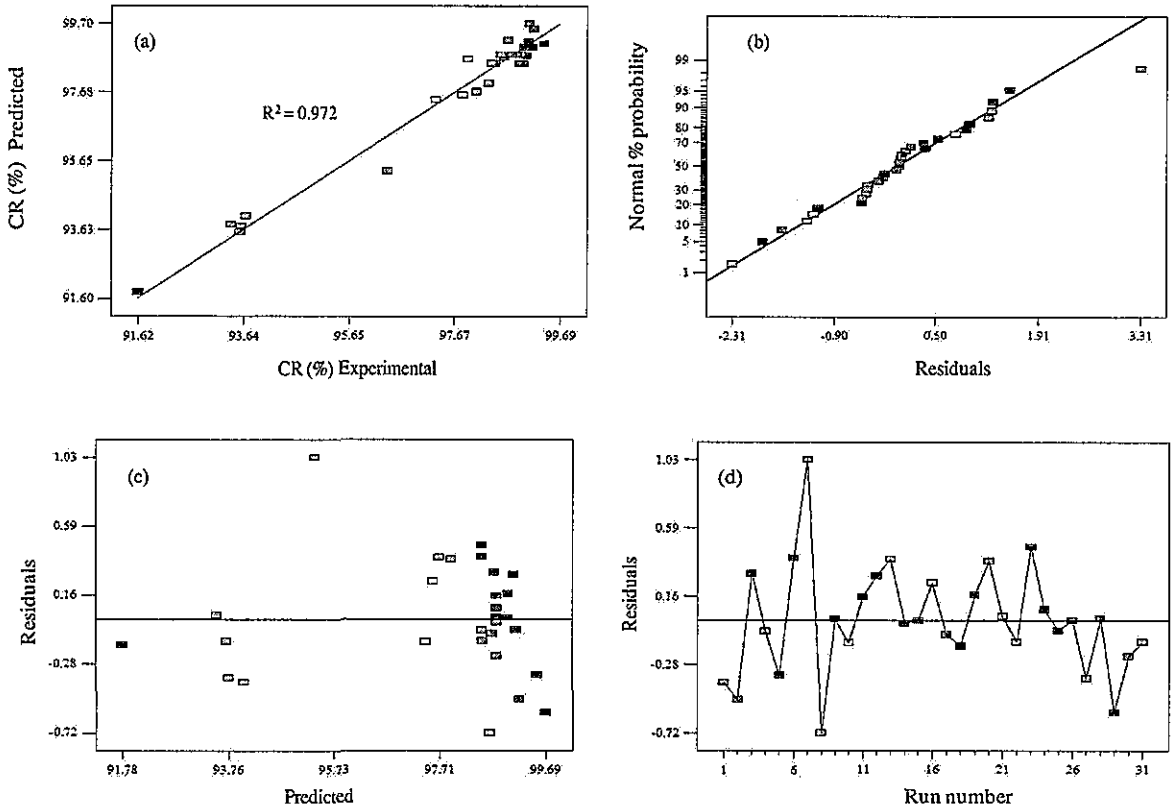

Figure 4. (a) Plot of predicted versus experimental color removal (CR (%)) and (b–d) corresponding residual plots.

(3D) response surface plots for the calculated response were obtained based on the quadratic model. The effect of the initial BY2 concentration on its removal (%) is illustrated in Figure 5, while the temperature and adsorbent dosage were kept constant at 40 °C and 0.8 g/L, respectively. As depicted in Figure 5, increasing the initial BY2 concentration from 20 to 100 mg/L resulted in decreasing BY2 removal (%). According to Eq. (1), this result can be confirmed by the negative value obtained for initial dye concentration ($-0.82x_1$), which indicated that the adsorption of BY2 is inversely proportional to the initial dye concentration. However, the dye removal (%) via the adsorption did not vary as the dye concentration increased from 20 to 40 mg/L. Decreasing BY2 removal (%) with increasing initial concentration of it is probably ascribed to the saturation of adsorptive sites placed on the surface of nanoclay.[40] This result can also be attributed to the aggregation of dye molecules at high concentration, which makes it impossible to diffuse into the adsorbent structure.[14] The contour plot and corresponding response surface plot of the effect of the adsorbent dosage on BY2 removal (%) are represented in Figure 6. As shown, the BY2 removal (%) increased with adsorbent dosage. However, increasing adsorbent dosage from 1.15 to 1.50 g/L led to a small decrease in BY2 removal (%). The increase in adsorbent dosage leads to increasing active adsorption sites. However, it can cause lowering of the concentration gradient between the adsorbent interface and the solution at constant adsorbate concentration, resulting in a small decrease in the adsorption at higher adsorbent concentrations.[41,42] Similar behavior was observed and reported by Silva et al. in their study on the adsorption of an industrial anionic dye by modified montmorillonite.[43] The interactive effect of the initial BY2 concentration and adsorbent dosage on CR (%) is depicted in Figure 7. In accordance

with Figures 5 and 6, Figure 7 shows the increase in BY2 removal (%) as the initial dye concentration decreased and adsorbent dosage increased. The effect of temperature on the CR (%) was studied, while the initial BY2 concentration and adsorbent dosage were kept constant at 60 mg/L and 0.8 g/L, respectively. Figure 8 shows that the change in the temperature caused no significant effect on the CR (%). This demonstrated that the adsorption of BY2 onto montmorillonite was independent of the temperature. As stated previously, the effect of temperature (F-value = 0.40) along with the contact time (F-value = 0.23) produced the lowest effect on the adsorption of BY2 in comparison with the other two variables. Moreover, as can be seen from Eq. (1), the negative value of temperature ($-0.063x_3$) indicated that increasing temperature causes a small drop in the adsorption of BY2. If the adsorption increases with increasing temperature then the adsorption is an endothermic process. Inversely, decreasing adsorption with increasing temperature implies that the adsorption is an exothermic process;[44] thus, the adsorption of BY2 onto nanoclay can be classified as an exothermic process. In contrast, Zhou et al. reported that dye adsorption onto cellulose acetate/organo-montmorillonite composites is temperature-dependent in which the increase in the temperature resulted in an increment in the adsorption.[41] The interactive effect of the temperature and adsorbent dosage on BY2 removal (%) is shown in Figure 9. As illustrated, the BY2 removal (%) increased with the adsorbent dosage irrespective of the change in the initial temperature. In addition, as it is obvious from Figures 5, 6, and 8, no significant increase in BY2 removal (%) happened as the reaction time increased to 45 min. This indicates a rapid adsorption of the dye onto the surface of the adsorbent and subsequently slow adsorption of the dye molecules into the pores.[15] This phenomenon can be clarified by the fact that the adsorption of BY2 onto nanoclay is a combination of rapid physical adsorption and subsequently a slow chemical adsorption.[45] A similar trend was observed and reported by other researchers in the case of the adsorption of Basic Red 46 onto a clay-like adsorbent.[46]

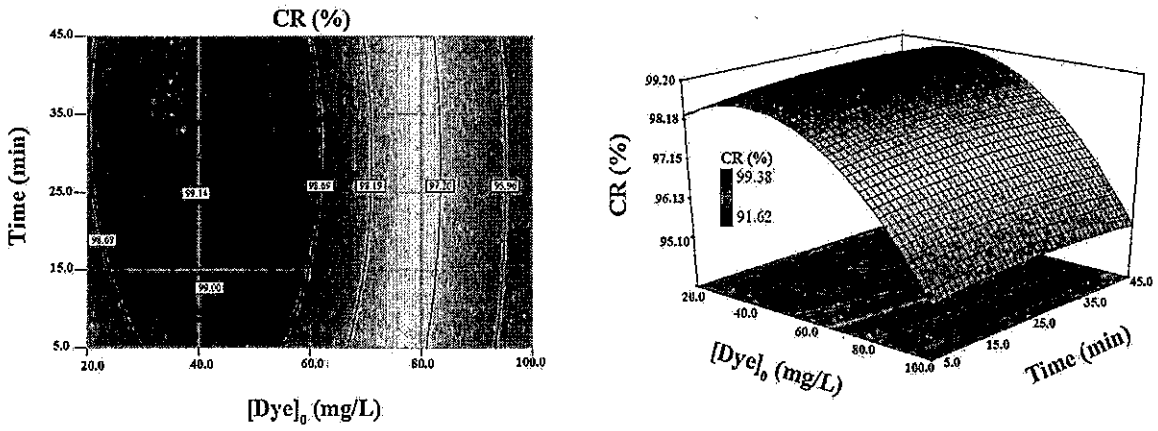

Figure 5. The contour plot and corresponding response surface plot for the BY2 removal as the function of initial dye concentration (mg/L) and reaction time (min).

2.4. Optimization through numerical optimization

Determining the optimum values for the variables influencing the BY2 removal by montmorillonite is the main goal of the optimization process. The desired response (CR (%)) was determined as "maximize" to attain the highest BY2 removal (%), while the independent variables were arranged to the full studied range. For maximum BY2 removal of 97.32%, the initial dye concentration, adsorbent dosage, reaction time, and temperature were

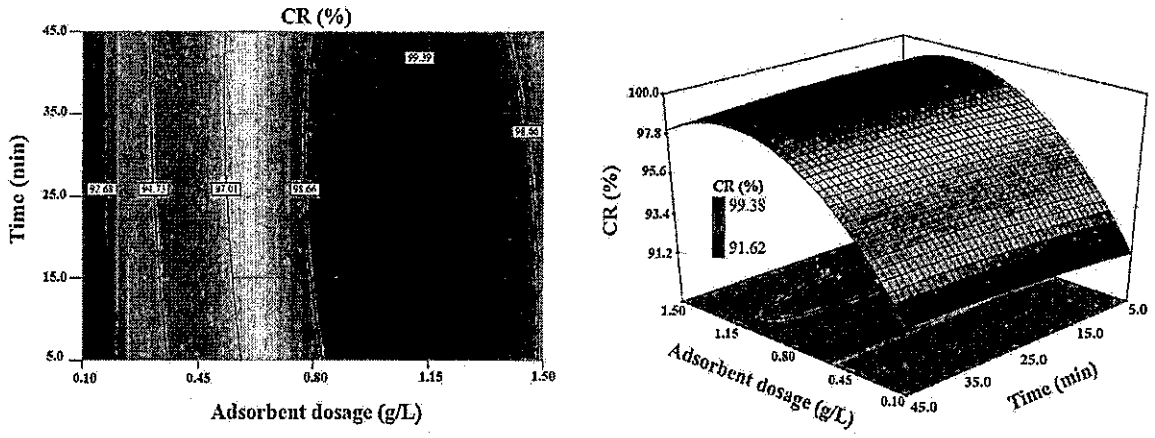

Figure 6. The contour plot and corresponding response surface plot for the BY2 removal as the function of adsorbent dosage (g/L) and reaction time (min).

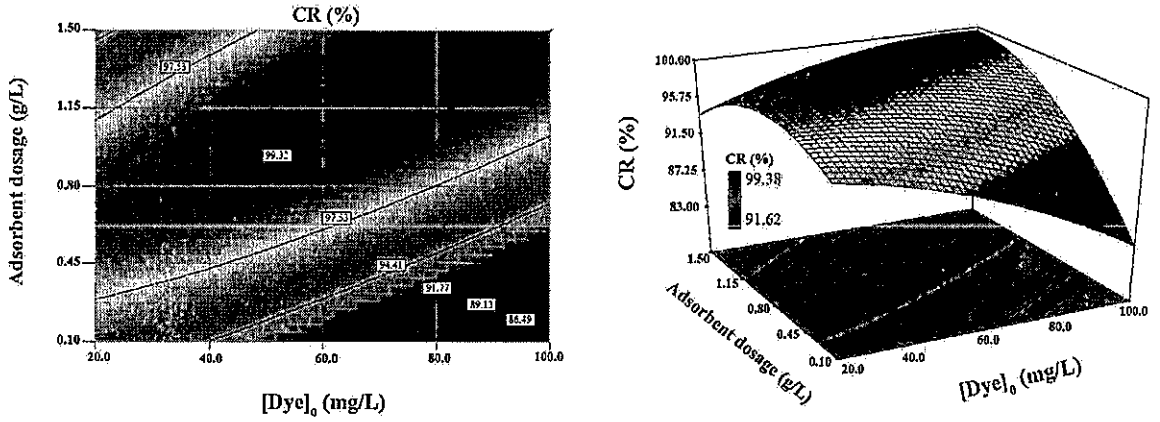

Figure 7. The contour plot and corresponding response surface plot for the BY2 removal as the function of initial dye concentration (mg/L) and adsorbent dosage (g/L).

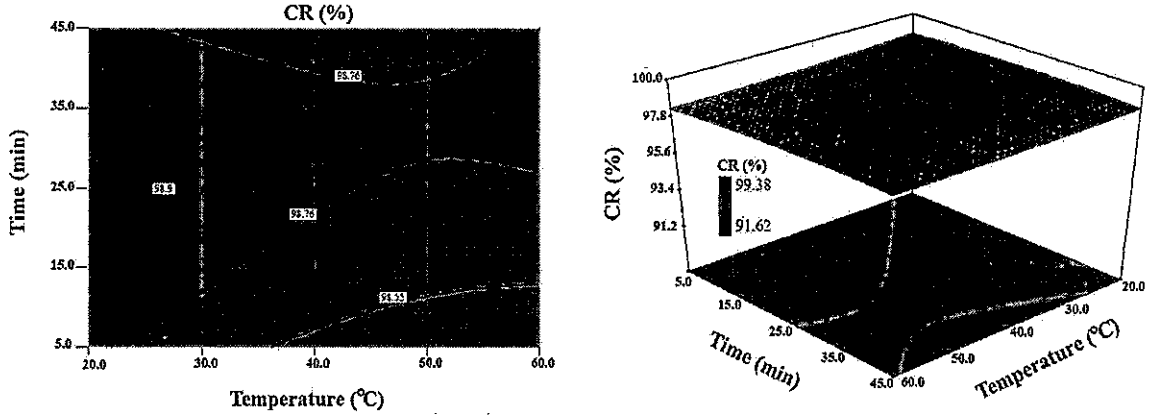

Figure 8. The contour plot and corresponding response surface plot for the BY2 removal as the function of temperature (°C) and reaction time (min).

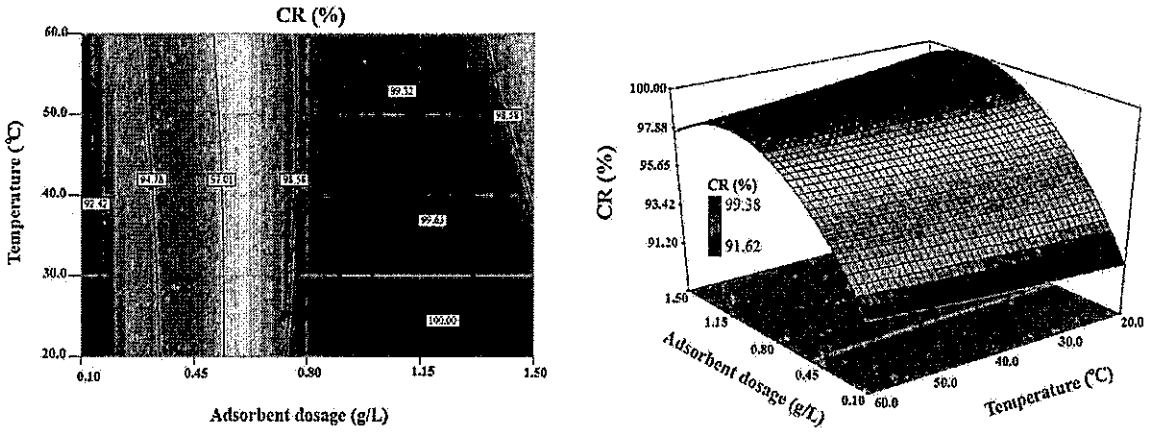

Figure 9. The contour plot and corresponding response surface plot for the BY2 removal as the function of adsorbent dosage (g/L) and temperature (°C).

obtained to be 60 mg/L, 0.6 g/L, 10 min, and 25 °C, respectively. To confirm the results of the optimization process, three additional experiments were carried out under optimized conditions. A mean experimental BY2 removal (%) of 98.28% demonstrated good agreement between the predicted and experimental BY2 removal. This indicated the validity of the model applied for the adsorption of BY2 onto montmorillonite.

2.5. Kinetic study

In order to describe the rate and mechanism of the BY2/MMT adsorption system at 25 °C and determine the factors controlling the rate of adsorption, three kinetic models including pseudo-first-order, pseudo-second-order, and intraparticle diffusion models were used with an initial concentration of 60 mg/L. The constant parameters and regression coefficients of the equations for this system were obtained by computing from the intercept and the slope of the plots using the linear form of the isotherm equations. The results are presented in Table 5, together with the linear forms of the kinetic equations. The obtained results in this study were not fitted with the pseudo-first-order model. As can be seen from Table 5, the pseudo-second-order kinetic model had the highest correlation coefficient ($R^2 = 1.00$), indicating that the adsorption of BY2 onto MMT surface followed the pseudo-second-order kinetic model. The high fitting for this equation showed the presence of chemical and strong electrostatic attractions between the functional groups of adsorbent and adsorbate molecules or an activated adsorption mechanism.[4,17] The adsorption kinetics of BY2 onto the MMT surface was also studied on the basis of the intraparticle diffusion model and the experimental data were fitted to the intraparticle diffusion model, indicating that the adsorption process occurred via a multistep mechanism involving exterior surface adsorption and subsequent intraparticle or pore diffusion.[4,17,47] Table 5 shows that the order of adsorption rate was the first stage (k_{i1}) < second stage (k_{i2}). The changes in k_{i1} and k_{i2} could be attributed to the adsorption stages of the exterior surface and interior surface, respectively. A plot of q_t versus $t^{1/2}$ for the equation of the intraparticle diffusion model did not pass through the origin. Therefore, it can be said that intraparticle diffusion is not the sole rate-determining step. As seen in Table 5, the low external diffusion rate (0.003 mg/min$^{1/2}$/g) for the adsorption of BY2 onto MMT was probably due to the heteroporous structure of the adsorbent, which decreased the diffusion rate.[47]

Table 5. The kinetic constants of pseudo-second-order and intraparticle diffusion models in the BY2 removal using adsorption onto montmorillonite.

Kinetic models	Equation	Parameters	Values
Pseudo-second-order	$t/q_t = 1/k_2 q_e^2 + t/q_e$	k_2(g/mg/min)	1.17
		q_e(mg/g)	92.59
		R^2	1.0000
Intraparticle diffusion	$q_t = k_p t^{1/2} + C$	k_1 (mg/min$^{1/2}$/g)	0.003
		R^2	0.9640
		k_2 (mg/min$^{1/2}$/g)	0.0625
		R^2	0.9524

k_p, Intraparticle diffusion constant; q_t, amount of adsorbed dye; C, intercept; k_2, rate constant of the pseudo-second order.

2.6. Isotherm study

In order to determine the mechanism of BY2 adsorption on the MMT surface, the experimental data were applied to the Freundlich and Langmuir isotherm equations, which are the most common models used in adsorption studies. The constant parameters of the equations for this system were calculated by regression using the linear form of the isotherm equations. The results, together with the isotherm equations, are given in Table 6; the Langmuir isotherm assumes the monolayer adsorption of adsorbate molecules without any interaction with each other on the adsorbent surface, with identical binding sites energetically.[48] As can be seen from Table 6, the adsorbent sample was fitted quite well into the Langmuir equation ($R^2 = 0.9389$). This fitting also indicated that the adsorption of dye occurred predominantly through the strong interactions. The shape of the Langmuir isotherm was examined by the dimensionless constant called the separation factor, R_L. $R_L = 1/1 + kC_o$, where k is the Langmuir constant, C_o is the initial BY2 concentration, and R_L values determine whether the type of isotherm is linear ($R_L = 1$), irreversible ($R_L = 0$), favorable ($0 < R_L < 1$), or unfavorable ($R_L > 1$).[17,48] The values of R_L for the adsorption of BY2 onto the MMT surface were between 0.02 and 0.094, indicating that the process had occurred favorably.[17,48] The Freundlich isotherm is an empirical equation derived by assuming a heterogeneous adsorbent surface with its adsorption sites being at varying energy levels.[4,17,48] By considering the high R^2 value ($R^2 = 0.9792$) obtained from the Freundlich model, it can be said that this model provides a better fit to the experimental data (see Table 6). In our study, when comparing the regression coefficient values for both Langmuir and Freundlich isotherms, it was demonstrated that the Freundlich isotherm was the most appropriate in describing the equilibrium data for dye adsorption at the studied temperature.

Table 6. Langmuir and Freundlich isotherm constants in the BY2 removal using adsorption onto montmorillonite.

Isotherm	Equation	Parameters	Values
Langmuir	$C/q = 1/kq_m + (1/q_m)\,C$	q_m (mg/g)	161.29
		k (L/mg)	0.48
		R^2	0.9389
Freundlich	lnq = lnk + nlnC	n	0.3317
		K_F ((mg/g)(L/mg)$^{1/n}$)	59.25
		R^2	0.9792

q, adsorption capacity of BY2 (mg/g); q_m, monolayer adsorption capacity; C, equilibrium concentration, n, k are constant parameters for the isotherm equations.

3. Experimental

3.1. Chemicals

The inorganic clay used in this study was K-10 grade montmorillonite purchased from Sigma–Aldrich Co. (USA) with a surface area of 279.27 m^2/g. The chemical composition (wt%) of the clay sample (main elements) was SiO_2: 66.9%, Al_2O_3: 13.8%, Fe_2O_3: 2.75%, MgO: 1.58% and other 14.97%. The cation-exchange capacity (CEC) of the clay is determined by the ammonium acetate method as 120 meq/100 g.[49] The BY2 ($C_{17}H_{22}ClN_3$, molecular weight 303.83 g/mol) used as a model diarylmethane dye was purchased from Shimi Boyakhsaz Company, Iran, and used without any purification. All chemicals used in the present investigation were of analytical grade and purchased from Merck, Germany.

3.2. Experimental procedure and analysis

To carry out the adsorption experiments, 100-mL glass-stoppered round-bottom flasks immersed in a thermostatic shaker bath were used. The initial pH was adjusted with concentrated HCl and NaOH solution and measured by a WTW inoLab pH meter (WTW Inc., Weilheim, Germany). The pH meter was standardized with buffers before every measurement. At the end of each experimental run, the supernatant was withdrawn and centrifuged for 5 min at 6000 min^{-1}. The residual BY2 in the solution was measured with a Varian Cary 100 UV spectrophotometer (Australia) at λ_{max} of 432 nm. The color removal (%) by adsorption onto montmorillonite and the amount of BY2 adsorbed by the montmorillonite were estimated through Eqs. (4) and (5), respectively.

$$\text{Color removal } (CR(\%)) = [1 - (C/C_o)] \times 100 \tag{4}$$

$$q = \frac{(C_0 - C_e)V}{M}, \tag{5}$$

where q is the adsorption capacity (mg/g); C_o, C, and C_e are the dye concentrations at time 0, t, and equilibrium concentrations of BY2 (mg/L); V is the volume of BY2 solution (L); and M is the total amount of montmorillonite (g). The chemical composition (wt%) of the nanoclay sample (main elements) was determined by Rigaku RIX-3000 X-ray fluorescence spectrometry (Rigaku Corporation, Japan). The X-ray diffraction (XRD) patterns of the samples were gained by a Philips X-ray diffractometer (XRD: STOE D-64295 Germany). The BET surface area of the clay was measured through N_2 adsorption at 77 K in the relative pressure range from 0.06 to 0.99 using a Micromeritics Gemini, Model 2385 (USA). The pore size distributions were deduced from N_2 adsorption isotherms using the BJH method. Before measurements, the sample was degassed for 15 h at 100 °C in the degas port of the adsorption analyzer. FT-IR spectra of montmorillonite samples before and after adsorption of C.I. Basic Yellow 2 (BY2) at 293 K were run on a PerkinElmer Model 1600 FT-IR (USA) spectrophotometer using KBr pellets. Each sample was finely ground with oven-dried spectroscopic grade KBr and pressed into a disk. All samples were oven-dried at 120 °C to remove physisorbed water. Then the spectra were recorded at a resolution between 400 and 4000 cm^{-1}.

3.3. Experimental design based on a CCD

RSM based on a CCD was used to optimize the removal of BY2 by adsorption onto montmorillonite nanoclay. In recent decades, RSM has been utilized to assess the interactive effects of different operational variables in various biochemical and chemical processes. For this reason, RSM is more practical than the conventional

one-factor-at-a-time strategy. To analyze the efficacy of the process for removing BY2 through RSM, Design-Expert (version 7.0.0) software was applied. The effect of four main variables influencing the color removal was evaluated: the initial dye concentration (mg/L), the adsorbent dosage (g/L), temperature (°C), and reaction time (min). The number of experiments was calculated through Eq. (6):

$$N = 2^k + 2k + x_0, \tag{6}$$

where N, k, and x_0 are the number of experiments, the number of variables, and the number of central points, respectively.[2,18,38] According to Eq. (5), the total number of experiments was obtained to be 31 ($k = 4$, $x_0 = 7$). The selected variables (X_i) were coded as x_i according to Eq. (6):

$$x_i = (x_i - x_0)/\delta x, \tag{7}$$

where x_0 and δx are the values of x_i at the center point and step change, respectively.[37,38,50] The ranges and levels of the selected variables are represented in Table 7. The mathematical relationship between the response (CR (%)) and the operational variables can be described through Eq. (8):

$$\begin{aligned} Y = {} & b_0 + b_1x_1 + b_2x_2 + b_3x_3 + b_4x_4 + b_{12}x_1x_2 + b_{13}x_1x_3 + b_{14}x_1x_4 + b_{23}x_2x_3 + b_{24}x_2x_4 \\ & + b_{34}x_3x_4 + b_{11}x_{12} + b_{22}x_{22} + b_{33}x_{32} + b_{44}x_{42}, \end{aligned} \tag{8}$$

where Y is the predicted response of CR (%) and b_0, b_i, b_{ij}, and b_{ii} are constant, the regression coefficients for linear effects, the regression coefficients for squared effects, and the regression coefficients for interaction effects, respectively. In addition, x_i and x_j are the coded values for the experimental variables.[37,38]

Table 7. Ranges and levels of variables for the adsorption of BY2 by a central composite design.

No.	Variable	Name	Variable level				
			-2 (α)	-1	0	$+1$	$+2$ (α)
1	X_1	Dye (mg/L)	20	40	60	80	100
2	X_2	Adsorbent dosage (g/L)	0.1	0.45	0.8	1.15	1.5
3	X_3	Temperature (°C)	20	30	40	50	60
4	X_4	Time (min)	5	15	25	35	45

4. Conclusions

In the present investigation, the applicability of montmorillonite nanoclay was considered for the adsorption of a cationic dye from aqueous solutions. To vigorously evaluate the efficacy of the studied adsorbent for removing BY2 from the aqueous phase under different operational conditions, a CCD was applied. The experimental design (31 runs) was obtained using Design-Expert software. The individual and interactive effects of four main operational parameters influencing the adsorption of BY2 were studied: initial dye concentration, adsorbent dosage, reaction time, and temperature. Accordingly, a quadratic model was developed to predict the BY2 removal efficiency in terms of individual and interactive effects of operational parameters. The quadratic model was analyzed using ANOVA. The F-value, P-value, and the value of sum of squares of the applied model were 40.73, 0.0001, and 133.08, respectively. This implies that the model can be considered an appropriate and reliable tool to correlate between the response and independent parameters. Three dimensional response surface plots and corresponding contour plots, which are simulated from the models, were applied to describe

the effect of studied parameters on the removal of BY2. Decreasing the initial BY2 concentration together with increasing adsorbent dosage resulted in increasing BY2 removal (%), while the change in reaction time and temperature caused an insignificant change in BY2 removal. The obtained correlation coefficient demonstrated a good agreement between the predicted and experimental results. For a maximized BY2 removal of 97.32%, the initial dye concentration, adsorbent dosage, reaction time, and temperature were 60 mg/L, 0.6 g/L, 10 min, and 25 °C, respectively. The result of FT-IR analysis confirms the involvement of O–H and N–H groups in the BY2 and montmorillonite interaction. Thus, montmorillonite clay would be an efficient adsorbent for the removal of BY2 dye from aqueous solutions. Finally, the results indicated that the CCD statistical approach is an appropriate tool to optimize the operational parameters for maximized removal efficiency.

Acknowledgments

The authors thank the University of Tabriz (Iran), Atatürk University in Erzurum (Turkey), and Arak University of Medical Sciences (Iran) for all support provided.

References

1. Noorimotlagh, Z.; Darvishi Cheshmeh Soltani, R.; Khataee, A. R.; Shahriyar, S.; Nourmoradi, H. *J. Taiwan Inst. Chem. Eng.* **2014**, *45*, 1783–1791.
2. Khataee, A. R.; Fathinia, M.; Aber, S.; Zarei, M. *J. Hazard. Mater.* **2010**, *181*, 886–897.
3. Gürses, A.; Doğar, Ç.; Yalçın, M.; Açıkyıldız, M.; Bayrak, R.; Karaca, S. *J. Hazard. Mater.* **2006**, *131*, 217–228.
4. Darvishi Cheshmeh Soltani, R.; Khataee, A. R.; Safari, M.; Joo, S. W. *Int. Biodeter. Biodegr.* **2013**, *85*, 383–391.
5. Darvishi Cheshmeh Soltani, R.; Rezaee, A.; Shams Khorramabadi, G.; Yaghmaeian, K. *Water Sci. Technol.* **2011**, *63*, 129–135.
6. Shams Khorramabadi, G.; Darvishi Cheshmeh Soltani, R.; Rezaee, A.; Khataee, A. R.; Jonidi Jafari, A. *Can. J. Chem. Eng.* **2012**, *90*, 1539–1546.
7. Uzun, İ.; Güzel, F. *Turk. J. Chem.* **2000**, *24*, 291–298.
8. Qadeer, R.; Rehan, A. H. *Turk. J. Chem.* **2002**, *26*, 357–362.
9. Gürses, A.; Doğar, Ç.; Karaca, S.; Açikyildiz, M.; Bayrak, R. *J. Hazard. Mater.* **2006**, *131*, 254–259.
10. Darvishi Cheshmeh Soltani, R.; Khataee, A. R.; Godini, H.; Safari, M.; Ghanadzadeh, M. J.; Rajaei, M. S. *Desalin. Water Treat.* **2014**, 1–14.
11. Gürses, A.; Karaca, S.; Açikyildiz, M.; Ejder, M. *Chem. Eng. J.* **2009**, *147*, 194–201.
12. Teng, M.-Y.; Lin, S.-H. *Desalination* **2006**, *201*, 71–81.
13. Wibulswas, R. *Sep. Purif. Technol.* **2004**, *39*, 3–12.
14. Wang, L.; Wang, A. *J. Hazard. Mater.* **2008**, *160*, 173–180.
15. Selvam, P. P.; Preethi, S.; Basakaralingam, P.; Thinakaran, N.; Sivasamy, A.; Sivanesan, S. *J. Hazard. Mater.* **2008**, *155*, 39–44.
16. Wang, C.-C.; Juang, L.-C.; Hsu, T.-C.; Lee, C.-K.; Lee, J.-F.; Huang, F.-C. *J. Colloid Interface Sci.* **2004**, *273*, 80–86.
17. Hassani, A.; Darvishi Cheshmeh Soltani, R.; Karaca, S.; Khataee, A. *J. Ind. Eng. Chem.* **2015**, *21*, 1197–1207.
18. Darvishi Cheshmeh Soltani, R.; Rezaee, A.; Khataee, A. R.; Godini, H. *Can. J. Chem. Eng.* **2014**, *92*, 13–22.
19. Darvishi Cheshmeh Soltani, R.; Rezaee, A.; Khataee, A. R.; Safari, M. *J. Ind. Eng. Chem.* **2014**, *20*, 1861–1868.
20. Karaca, S.; Gürses, A.; Ejder Korucu, M. *J. Chem.* **2013**, *2013*, 1–10.

21. Khataee, A.; Sheydaei, M.; Hassani, A.; Taseidifar, M.; Karaca, S. *Ultrason. Sonochem.* **2015**, *22*, 404–411.
22. Rouquerol, J.; Avnir, D.; Everett, D. H.; Fairbridge, C.; Haynes, M.; Pernicone, N.; Ramsay, J. D. F.; Sing, K. S. W.; Unger, K. K. *Stud. Surf. Sci. Catal.* **1994**, *87*, 1–9.
23. Sing, K. S. W.; Everett, D. H.; Haul, R. A. W.; Moscou, L.; Pierotti, R. A.; Rouquerol, J.; Siemieniewska, T. *Pure Appl. Chem.* **1985**, *57*, 603–619.
24. Sing, K. S. W.; Everett, D. H.; Haul, R. A. W.; Moscou, L.; Pierotti, R. A.; Rouquerol, J.; Siemieniewska, T. In *Handbook of Heterogeneous Catalysis, Vol. 2*; 2nd ed.; Ertl, G., Knözinger, H., Schüth, F., Weitkamp, J., Eds. Wiley-VCH Verlag GmbH& Co: Weinheim, Germany, 2008.
25. Barrett, E. P.; Joyner, L. G.; Halenda, P. P. *J. Am. Chem. Soc.* **1951**, *73*, 373–380.
26. Brunauer, S.; Deming, L. S.; Deming, W. E.; Teller, E. *J. Am. Chem. Soc.* **1940**, *62*, 1723–1732.
27. Darvishi Cheshmeh Soltani, R.; Rezaee, A.; Khataee, A. *Ind. Eng. Chem. Res.* **2013**, *52*, 14133–14142.
28. Darvishi Cheshmeh Soltani, R.; Safari, M.; Rezaee, A.; Godini, H. *Environ. Progr. Sustain. Energ.* **2015**, *34*, 105–111.
29. Chen, D.; Chen, J.; Luan, X.; Ji, H.; Xia, Z. *Chem. Eng. J.* **2011**, *171*, 1150–1158.
30. Wu, P.; Wu, W.; Li, S.; Xing, N.; Zhu, N.; Li, P.; Wu, J.; Yang, C.; Dang, Z. *J. Hazard. Mater.* **2009**, *169*, 824–830.
31. Patel, H. A.; Somani, R. S.; Bajaj, H. C.; Jasra, R. V. *Appl. Clay Sci.* **2007**, *35*, 194–200.
32. Wu, Z.; Joo, H.; Ahn, I.-S.; Haam, S.; Kim, J.-H.; Lee, K. *Chem. Eng. J.* **2004**, *102*, 277–282.
33. Al-Ghouti, M. A.; Al-Degs, Y. S. *Chem. Eng. J.* **2011**, *173*, 115–128.
34. Öztürk, A.; Malkoc, E. *Appl. Surf. Sci.* **2014**, *299*, 105–115.
35. Khataee, A. R.; Zarei, M.; Moradkhannejhad, L. *Desalination* **2010**, *258*, 112–119.
36. Haber, A.; Runyun, R. *General Statistics*; 3rd edn. Boston, MA, USA: Addison-Wesley, 1977.
37. Khataee, A. R.; Zarei, M.; Asl, S. K. *J. Electroanal. Chem.* **2010**, *648*, 143–150.
38. Darvishi Cheshmeh Soltani, R.; Rezaee, A.; Godini, H.; Khataee, A. R.; Hasanbeiki, A. *Chem. Ecol.* **2012**, *29*, 72–85.
39. Khataee, A. R.; Kasiri, M. B.; Alidokht, L. *Environ. Technol.* **2011**, *32*, 1669–1684.
40. Deniz, F.; Saygideger, S. D. *Desalination* **2010**, *262*, 161–165.
41. Zhou, C.-H.; Zhang, D.; Tong, D.-S.; Wu, L.-M.; Yu, W.-H.; Ismadji, S. *Chem. Eng. J.* **2012**, *209*, 223–234.
42. Ghorbani, F.; Younesi, H.; Ghasempouri, S. M.; Zinatizadeh, A. A.; Amini, M.; Daneshi, A. *Chem. Eng. J.* **2008**, *145*, 267–275.
43. Silva, M. M. F.; Oliveira, M. M.; Avelino, M. C.; Fonseca, M. G.; Almeida, R. K. S.; Silva Filho, E. C. *Chem. Eng. J.* **2012**, *203*, 259–268.
44. Salleh, M. A. M.; Mahmoud, D. K.; Karim, W. A. W. A.; Idris, A. *Desalination* **2011**, *280*, 1–13.
45. Hu, B.; Luo, H. *Appl. Surf. Sci.* **2010**, *257*, 769–775.
46. Sheshdeh, R. K.; Nikou, M. R. K.; Badii, K.; Limaee, N. Y.; Golkarnarenji, G. *J. Taiwan Inst. Chem. Eng.* **2014**, *45*, 1792–1802.
47. Karaca, S.; Gürses, A.; Ejder, M.; Açıkyıldız, M. *J. Colloid Interface Sci.* **2004**, *277*, 257–263.
48. de Luna, M. D. G.; Flores, E. D.; Genuino, D. A. D.; Futalan, C. M.; Wan, M.-W. *J. Taiwan Inst. Chem. Eng.* **2013**, *44*, 646–653.
49. Madeira, M.; Auxtero, E.; Sousa, E. *Geoderma* **2003**, *117*, 225–241.
50. Khataee, A. R.; Dehghan, G. *J. Taiwan Inst. Chem. Eng.* **2011**, *42*, 26–33.